

- scribed in detail in R. Müller *et al.*, *Geophys. Res. Lett.* **21**, 1427 (1994). The most important of the more than 100 reactions used in the model are listed in Table 1.
15. W. B. DeMore *et al.*, *JPL Publication 92-20*, Jet Propulsion Laboratory, Pasadena, CA (1992).
 16. WMO/UNEP, Report Number 16, World Meteorological Organization, Geneva (1986).
 17. This surplus was significantly enhanced in the region below 45 km in model runs (not shown) where we included a 5% yield of HCl in reaction between ClO and OH, following suggestions of R. Toumi and S. Bekki [*Geophys. Res. Lett.* **20**, 2447 (1993)], and S. Chandra *et al.* (*ibid.*, p. 351).
 18. K. Minschwaner, R. J. Salawitch, M. B. McElroy, *J. Geophys. Res.* **98**, 10543 (1993). If we assume that our O₂ photolysis rate is 10% too high, a possibility that cannot be excluded from a recent model inter-comparison, the computed O₃ surplus (above about 45 km) is reduced to about 5%.
 19. Further calculations were performed for other latitudes and situations like HALOE sunrise and sunset

- coincidences near 20°N in the winter hemisphere. Similar results were obtained.
20. The calculated ClO concentrations are in accordance with the ClO observations by the Microwave Limb Sounder (MLS) instrument aboard UARS for the same day, taken at around 8:00 am local time. The uncertainty range of the MLS data is, however, large.
 21. HALOE O₃ observations have been validated against ozone sondes, lidars, ground-based microwave sounders, a rocket sonde, and different balloon-borne optical instruments [C. Brühl *et al.*, unpublished results]. Below ≈35 km, there is typically agreement within 5%, whereas above this level it is within 10%. However, the HALOE O₃ measurements appear to be systematically lower than correlative measurements by about 5% near the stratopause. In the intercomparisons with other satellite instruments (the Stratospheric Aerosol and Gas Experiment and the Solar and Backscatter Ultraviolet Spectrometer), similar differences were found.
 22. J. E. Harries *et al.*, unpublished results.

23. L. L. Gordley *et al.*, unpublished results.
24. J. M. Russell *et al.*, unpublished results.
25. R. T. Clancy *et al.*, *J. Geophys. Res.* **99**, 5465 (1994).
26. If this rate constant is reduced by 1σ (48%), it is approximately equal to the one recommended earlier [JPL Publication 83-62, Jet Propulsion Laboratory, Pasadena, CA (1983)], which was used in older studies.
27. J. C. Gille and J. M. Russell III, *J. Geophys. Res.* **89**, 5125 (1984); E. E. Remsburg *et al.*, *ibid.*, p. 5161.
28. M. R. Gunson *et al.*, *ibid.* **95**, 13867 (1990).
29. S. Solomon *et al.*, *ibid.* **91**, 9865 (1986); B. J. Connor *et al.*, *ibid.* **99**, 16757 (1994).
30. A reevaluation of LIMS NO₂ indicates that these NO₂ data are systematically too high by up to 20% [E. E. Remsburg *et al.*, *J. Geophys. Res.* **99**, 22965 (1994)].
31. We thank D. Lary for helpful comments on the calculation of the photolysis rates.

15 December 1994; accepted 27 February 1995

Global Mean Sea Level Variations from TOPEX/POSEIDON Altimeter Data

R. S. Nerem

The TOPEX/POSEIDON satellite altimeter mission has measured global mean sea level every 10 days over the last 2 years with a precision of 4 millimeters, which approaches the requirements for climate change research. The estimated rate of sea level change is $+3.9 \pm 0.8$ millimeters per year. A substantial portion of this trend may represent a short-term variation unrelated to the long-term signal expected from global warming. For this reason, and because the long-term measurement accuracy requires additional monitoring, a longer time series is necessary before climate change signals can be unequivocally detected.

The measurement of a long-term rise in global mean sea level would provide important corroboration of predictions by climate models of global warming as a result of an increase in the "greenhouse" gases (1-3). The largest contributors to global sea level change caused by global warming are expected to be the melting of continental glaciers and polar ice (4) and the thermal expansion of the oceans (5). Climate models used to assess the effects of increased greenhouse gases in the atmosphere predict an increase in global mean air temperature of 1° to 4°C over the next century, which in turn would lead to global mean sea level changes of 30 to 50 cm (1, 6).

Global sea level change has typically been estimated from tide gauge measurements collected over the last century (7). However, tide gauges may move vertically as a result of postglacial rebound (8), tectonic uplift, and subsidence caused by underground fluid removal at rates comparable to the sea level change signal; tide gauges also have limited spatial distribution (9, 10). Therefore, long-term averaging is required to overcome these limitations (11).

After allowing for postglacial rebound of the mantle (8), most recent estimates of the observed global sea level rise over the last century range from 1.7 to 2.4 mm/year (11-13).

Satellite altimeter measurements combined with a precisely known spacecraft orbit should provide improved measurements of global sea level change over shorter periods because of their near global coverage and because they measure sea level relative to a precise reference frame whose origin coincides with the Earth's center of mass. Measurement errors for previous missions such as Seasat (1978), Geosat (1985 to 1989), and ERS-1 (1991 to present) were too large to detect the small changes in global mean sea level (14-16). The main errors were in determining the satellite's altitude, the ionosphere delay correction, the wet troposphere delay correction, and the long-term integrity of the radar instrument calibration.

For the United States-France TOPEX/POSEIDON (T/P) satellite, launched on 10 August 1992, many of these errors were greatly reduced (17): The orbit altitude precision has been improved to 3 to 4 cm root mean square (rms) with the use of SLR (satellite laser ranging) and DORIS (Dopp-

ler orbitography integrated by satellite) tracking data and improved satellite force models (18, 19); an ionosphere correction is produced directly from the dual frequency altimeter measurements (20); a wet troposphere correction is provided by on-board microwave radiometer measurements of the integrated water column (21); and the altimeter system calibration is monitored at two ground verification sites (22). The T/P satellite is in a near circular orbit at an altitude of 1336 km that is inclined to the equator at an angle of 66.06°, thus defining the latitudinal coverage of the measurements. The ground track repeats every 10 days and has a maximum cross-track spacing of 316 km at the equator (17). The T/P data have an absolute point-to-point accuracy of better than 5 cm (17). Because orbit altitude errors can be geographically correlated, even better accuracy is obtained for the measurement of sea level changes over 10-day intervals, with the data agreeing with island tide gauges at the 2-cm rms level (23, 24).

There are two radar altimeters on board T/P: a dual-frequency altimeter, which operates 90% of the time, and an experimental, solid-state single-frequency altimeter, which operates the remaining time. Data from both altimeters were used in this study (25). The radar altimeters collect 10 measurements per second, but 1-s averages were used in this study, which yields about a half-million measurements every 10 days. These measurements have been corrected for the effects of ionospheric path delay, dry-wet troposphere delay, and variable sea state. The resulting sea level variations have also had tidal effects removed, including the solid Earth tides, the ocean tides (26), and the ocean tidal loading. Sea level variations caused by variations in air pressure loading (the "inverted barometer" effect) were not removed because it is the total sea level signal that is of interest, and globally, the current model for this correc-

NASA/Goddard Space Flight Center, Space Geodesy Branch, Code 926, Greenbelt, MD 20771, USA.

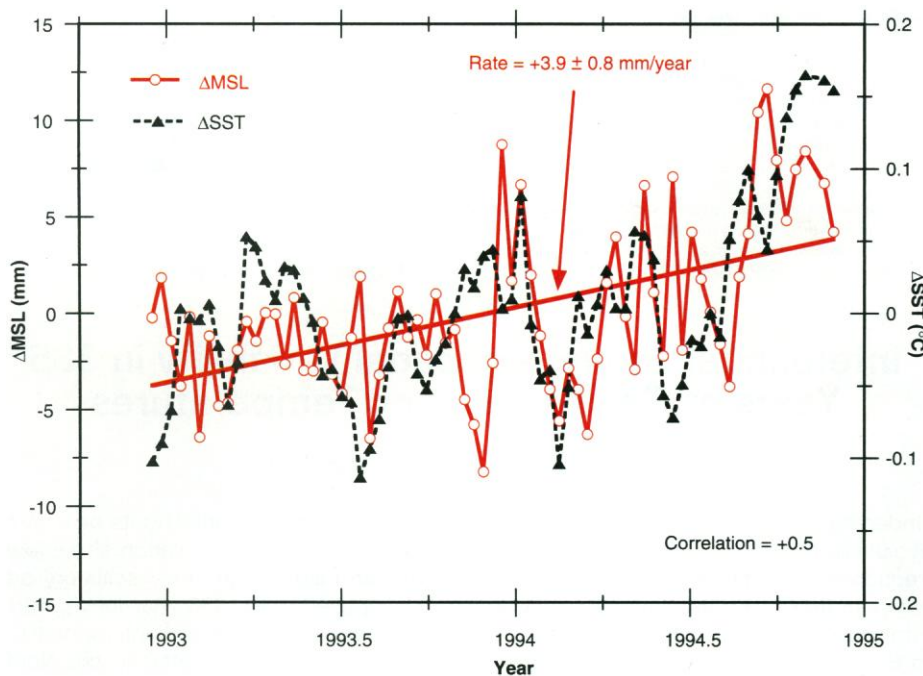


Fig. 1. Global mean sea level variations computed for each 10-day cycle of T/P altimetry covering cycles 9 through 81 (11 December 1992 to 5 December 1994), except for cycle 79, which was unavailable as of this writing. Also shown are global mean SST anomalies covering the same time period, derived from the weekly 1° by 1° SST fields of the National Meteorological Center (33, 34).

tion does not conserve oceanic mass. After editing suspect data (27), mean sea level variations were computed by averaging the local sea level variations within each 10-day repeat cycle over all observed latitudes and longitudes. Because the altimeter data are unequally distributed in latitude, a latitude-dependent weighting factor was applied so that each area of the ocean contributed equally to the determination of mean sea level.

The stability of the altimeter instrument calibration is of significant concern for studies of mean sea level change because the instrument can drift with time as the hardware ages. For this study, calibration results derived from on-board internal instrument measurements were adopted (28, 29). They show a shortening of the altimeter range measurement of 2.8 mm/year over the first 2 years of the mission; thus, this calibration has significantly reduced the sea level rise estimate. This internal calibration assesses only the altimeter electronics and not the supporting measurement corrections; corroboration of the observed drift by the ground calibration sites is still needed. The results from the official ground calibration sites (22), as well as comparisons to tide gauge data (23), are inconclusive but will improve with further monitoring.

The data analyzed in this study covers T/P repeat cycles 9 to 81, corresponding to 11 December 1992 to 5 December 1994. The first 80 days of the mission data were

eliminated because the data are suspect (30). The time series of 10-day global mean sea level variations after correction for the instrument drift is shown in Fig. 1. There was no significant change when data above $\pm 55^\circ$ latitude were eliminated; thus, the results are probably not greatly affected by the lack of coverage above $\pm 66^\circ$. Satellite altitude error is not a large contributor to errors in the time series, as the results were not greatly affected by the use of independent orbit solutions computed with tracking data from an experimental on-board Global Positioning System (GPS) receiver (31). The use of an alternative ionosphere correction, derived from the DORIS tracking data, also did not greatly affect the time series, indicating that errors in this relatively large measurement correction are not a major concern.

The mean sea level variations shown in Fig. 1 have a standard deviation of 4 mm, nearly a factor of 5 better than previous missions (14–16). A spectral analysis of the sea level variations shows millimeter-level signals at periods of 30, 52, 63, 89, and 127 days but no significant seasonal variations, although the annual heating cycle is clearly seen if the Northern and Southern Hemispheres are evaluated independently (24). A linear least-squares fit to the variations gives a rate of sea level rise of $+3.9 \pm 0.8$ mm/year, where the predicted error is a “noise”-only estimate based solely on the variance of the time series. It is difficult to provide absolute error estimates for the

mean sea level variations because this requires a detailed understanding of the characteristics of the contributing errors to unprecedented levels. The local rate of sea level change varies geographically by ± 40 mm/year mainly because of the current El Niño–Southern Oscillation (ENSO) event. The detection of spatial variations in the long-term signal of sea level rise will require a considerably longer time series acquired from multiple satellite missions comparable to T/P.

It is quite possible that the mean sea level variations shown in Fig. 1 are real, and thus, they were compared to coincident global mean sea surface temperature (SST) anomalies because of the importance of upper ocean heat content on steric sea level (32). Weekly 1° by 1° SST fields produced by the National Meteorological Center (NMC) (33) were used to compute global mean SST anomalies (34) (Fig. 1). Both time series generally increase over the T/P mission. As expected, the two time series share many common features, such as the short-term increase in sea level and SST seen near the end of 1993, although the correlation of the two time series is only +0.5. A spectral analysis of the SST anomalies shows signals with amplitudes of 0.01°C and periods of 31, 59, 87, and 119 days, similar to the sea level variations. Because sea level responds to temperature variations throughout the water column (though mainly in the top mixing layer), the level of agreement is quite encouraging and supports the idea that a significant portion of the observed variations in mean sea level arise from variations in upper ocean heat content. An examination of the entire 13-year SST time series (1982 to the present) (35) shows that the largest observed SST anomalies coincide with the occurrence of ENSO episodes. Therefore, the recent rise in global mean sea level might be attributable to both the current ENSO event and the long-term signal expected from global warming; thus, the importance of collecting a longer time series must be emphasized. It is also worth noting that most of the observed sea level rise occurs during the second year of the time series.

The estimated rate of mean sea level rise of $+3.9 \pm 0.8$ mm/year during 1993 to 1994 (36) is somewhat larger than the historical tide gauge estimates of sea level rise (1); however, considerably more altimeter data are required before the global warming signal can be separated from the short-term sea level variations. In September 1995, T/P will complete its nominal 3-year mission, but an extended mission of three additional years is anticipated. Nevertheless, T/P demonstrates the precision necessary to detect variations in global mean sea level caused by changes in the Earth’s climate.

REFERENCES AND NOTES

- J. T. Houghton, G. J. Jenkins, J. J. Ephraums, Eds., *Climatic Change: The IPCC Scientific Assessment* (Cambridge Univ. Press, Cambridge, 1990).
- J. T. Houghton, B. A. Callander, S. K. Varney, Eds., *Climate Change 1992: The Supplementary Report to the IPCC Scientific Assessment* (Cambridge Univ. Press, Cambridge, 1992).
- R. A. Warrick, E. M. Barrow, T. M. L. Wigley, Eds., *Climate and Sea Level Change: Observations, Projections, and Implications* (Cambridge Univ. Press, Cambridge, 1993).
- M. F. Meier, *Science* **226**, 1418 (1984).
- J. A. Church, J. S. Godfrey, D. R. Jacket, T. J. MacDougal, *J. Clim.* **4**, 438 (1991).
- T. M. L. Wigley, *Geophys. Res. Lett.* **22**, 45 (1995).
- K. O. Emery and D. G. Aubrey, *Sea Levels, Land Levels, and Tide Gauges* (Springer-Verlag, New York, 1991).
- A. M. Tushingham and W. R. Peltier, *J. Geophys. Res.* **96**, 4497 (1991).
- T. P. Barnett, *ibid.* **89**, 7980 (1984).
- M. Groger and H.-P. Plag, *Global Planet. Change* **8**, 161 (1993).
- B. C. Douglas, *J. Geophys. Res.* **96**, 6981 (1991).
- W. R. Peltier and A. M. Tushingham, *Science* **244**, 806 (1989).
- A. Trupin and J. Wahr, *Geophys. J. Int.* **100**, 441 (1990).
- G. H. Born, B. D. Tapley, J. C. Ries, R. H. Stewart, *J. Geophys. Res.* **91**, 11775 (1986).
- B. D. Tapley, C. K. Shum, J. C. Ries, R. Suter, B. E. Schutz, in *Sea Level Changes: Determination and Effects*, P. Woodworth, Ed. (American Geophysical Union, Washington, DC, 1992), vol. 11, pp. 167–180.
- C. A. Wagner and R. E. Cheney, *J. Geophys. Res.* **97**, 15607 (1992).
- L.-L. Fu *et al.*, *ibid.* **99**, 24369 (1994).
- B. D. Tapley *et al.*, *ibid.*, p. 24383.
- R. S. Nerem *et al.*, *ibid.*, p. 24421.
- D. A. Imel, *ibid.*, p. 24895.
- C. S. Ruf, S. J. Keihm, B. Subramanya, M. A. Janssen, *ibid.*, p. 24915.
- E. J. Christensen *et al.*, *ibid.*, p. 24465.
- G. T. Mitchum, *ibid.*, p. 24541.
- R. S. Nerem, E. J. Schrama, C. J. Koblinsky, B. D. Beckley, *ibid.*, p. 24565.
- The inclusion of the single-frequency altimeter data, which requires the use of an ionosphere correction computed from the DORIS tracking data, did not significantly change the results and thus were included for completeness.
- E. J. O. Schrama and R. D. Ray, *J. Geophys. Res.* **99**, 24799 (1994).
- In addition to the removal of data outliers, altimeter data in shallow water (<200 m) and inland seas have been omitted because of tide model uncertainties. Also, a specific location was excluded if the tidally corrected variability of the sea surface was greater than 40 cm rms or if there were less than 40 10-day data points in the time series. The measured global mean sea level variations were insensitive to changes in these criteria.
- G. S. Hayne, D. W. Hancock, C. L. Purdy, *TOPEX/POSEIDON Research News: JPL 410-42* **3**, 18 (1994).
- The calibration factor was applied only to the dual-frequency altimeter data; a calibration factor was previously applied to the single-frequency altimeter data by the instrument engineers (25).
- The first 80 days of T/P altimeter data, which are considered anomalous because of spacecraft pointing problems, show a decline of mean sea level of roughly 30 mm that has not been independently verified. However, if these data are included in the analysis presented here, the rate of mean sea level rise over the entire data set is reduced from +3.9 to -1.1 mm/year.
- W. I. Bertiger *et al.*, *J. Geophys. Res.* **99**, 24449 (1994).
- A. E. Gill and P. P. Niiler, *Deep-Sea Res.* **20**, 141 (1973).
- R. W. Reynolds and T. S. Smith, *J. Clim.* **7**, 929 (1994).
- Global mean SST anomalies were computed by temporally interpolating the weekly 1° by 1° NMC SST fields to the altimeter measurement times, removing the annual and semiannual variations averaged over 1982 to 1994, and then averaging the residuals between ±66° latitude with an equi-area weighting factor.
- R. W. Reynolds and D. C. Marsico, *J. Clim.* **6**, 115 (1993).
- Several members of the TOPEX/POSEIDON Science Team have computed a similar rate of sea level rise from the altimeter data, including Minster [J. F. Minster, C. Brossier, P. Rogel, *Eos* **75**, 56 (1994)], Rapp [R. H. Rapp, Y. Yi, Y. M. Wang, *J. Geophys. Res.* **99**, 24657 (1994)], and Wagner [C. A. Wagner *et al.*, *Eos* **75**, 56 (1994)].
- I thank B. D. Beckley, W. I. Bertiger, P. S. Callahan, E. J. Christensen, L. Fu, B. J. Haines, D. W. Hancock, G. S. Hayne, C. J. Koblinsky, G. Mitchum, K. E. Rachlin, R. H. Rapp, R. D. Ray, E. J. Schrama, and J. Wahr for their comments and contributions. This work was supported by a National Aeronautics and Space Administration TOPEX Project Science Investigation.

27 December 1994; accepted 1 March 1995

Interannual and Interdecadal Variability in 335 Years of Central England Temperatures

G. Plaut, M. Ghil,* R. Vautard

Understanding the natural variability of climate is important for predicting its near-term evolution. Models of the oceans' thermohaline and wind-driven circulation show low-frequency oscillations. Long instrumental records can help validate the oscillatory behavior of these models. Singular spectrum analysis applied to the 335-year-long central England temperature (CET) record has identified climate oscillations with interannual (7- to 8-year) and interdecadal (15- and 25-year) periods, probably related to the North Atlantic's wind-driven and thermohaline circulation, respectively. Statistical prediction of oscillatory variability shows CETs decreasing toward the end of this decade and rising again into the middle of the next.

Low-frequency climate variability, interannual and interdecadal, has been attributed to changes in the oceans' thermohaline circulation (THC) or wind-driven circulation. Multiple equilibria have been found in both THC (1) and wind-driven circulation (2) models. THC oscillates on scales of decades to millennia (3), whereas wind-driven oscillations are seasonal (4) or interannual (5). The strongest interannual climate signal is associated with the tropical El Niño–Southern Oscillation (ENSO) (6). The ENSO does have global effects (7), but their details are fairly uncertain at present (8). To determine the extent to which extratropical oceanic phenomena or ENSO affect climate variability in the northern mid-latitudes, we examined the CET record (9), the longest continuous instrumental temperature record.

Interdecadal and interannual oscillations have been recognized (10–13) in global or hemispheric temperature series of shorter duration (14–16) by two independent statistical techniques: singular-spectrum analysis (SSA) (10, 12, 17–19) and the multitaper method (11, 20). Given the

shortness of the series, these earlier results are still controversial (21, 22). The CET record (9, 23) now covers 335 years of averaged monthly temperatures, starting in January 1659 (24). Analysis of the CET record should thus settle this controversy, help determine the plausible causes of the peaks that have been detected, and permit a first glimpse at the secular variations of interdecadal variability.

To facilitate comparison with global and hemispheric analyses (10–13, 20–22), we performed SSA on the yearly averages of the CET record (23, 25). High-frequency interannual variability, such as a quasi-biennial oscillation (26), stands out when the monthly, rather than annual, CET data are analyzed with a wide enough SSA window (not shown); this variability is often related to ENSO (6, 27). We concentrate here on periods of 5 years and longer; use of a 1-year sampling interval and $M = 40$ lags (17) permits the study of periods between 5 and 40 years (19). Resolution increases with M , whereas statistical significance decreases. Window widths between 30 and 60 years gave similar results.

A break appears in the singular-spectrum slope (Fig. 1A) at order $k = 11$. A nonparametric Monte Carlo significance test (19) confirmed that the record's statistical dimension is $S = 11$ (28). The first two empirical orthogonal functions (EOFs) (Fig. 1B) are a data-adaptive running mean and its antisymmetric counterpart (10, 27). Eigenvalues 3 to 11 form four pairs (skip-

G. Plaut, Institut Non-Linéaire de Nice, 1361 route des Lucioles, F-06560 Valbonne, France.

M. Ghil, Department of Atmospheric Sciences and Institute of Geophysics and Planetary Physics, University of California, Los Angeles, CA 90095, USA.

R. Vautard, Laboratoire de Météorologie Dynamique du Centre National de la Recherche Scientifique, Ecole Normale Supérieure, 24 rue Lhomond, F-75231 Paris Cedex 5, France.

*To whom correspondence should be addressed.